Synthesis and Spectroscopic Characterization of *O*-Alkyl Dithiocarbonate (Xanthate) Derivatives of Dimethyl- and Diphenyltellurium(IV). Crystal Structures of $Me_2Te[S_2COEt]_2$ and $Ph_2Te[S_2COEt]_2$

Jane H. E. Bailey,† John E. Drake,* Layla N. Khasrou, and Jincai Yang

Department of Chemistry and Biochemistry, University of Windsor, Windsor, Ontario, Canada N9B 3P4

Received July 7, 1994[⊗]

Two series of *O*-alkyl dithiocarbonate (xanthate) derivatives of dimethyl- and diphenyltellurium(IV), $Me_2Te[S_2COR]_2$ and $Ph_2Te[S_2COR]_2$, where R = Me, Et, *i*-Pr, *n*-Pr, and *n*-Bu, have been prepared in 60−71% yields by the reaction of the potassium salt of the appropriate dithiocarbonic (xanthic) acid with dichlorodimethyltellurium(IV). The products were characterized principally by infrared, Raman, and ^1H, ^{13}C, and ^{125}Te NMR spectroscopy. The crystal structures of $Me_2Te[S_2COEt]_2$ and $Ph_2Te[S_2COEt]_2$ were determined. $Me_2Te[S_2COEt]_2$ (**2**) crystallizes in space group ($P\bar{1}$, No. 2) with the cell parameters a = 10.588(2) Å, b = 11.974(2) Å, c = 6.458(3) Å, α = 104.06(3)°, β = 90.67(2)°, γ = 71.25(1)°, V = 770.2(8)Å^3, and Z = 2; R = 0.0310, R_w = 0.0286. $Ph_2Te[S_2COEt]_2$ (**7**) also crystallizes in space group ($P\bar{1}$, No. 2) with the cell parameters a = 11.320(3) Å, b = 13.062(4) Å, c = 8.225(4)Å, α = 107.88(3)°, β = 110.72(3)°, γ = 79.91(3)°, V = 1078.3(8) Å^3, and Z = 2; R = 0.0366, R_w = 0.0329. The immediate environment about tellurium in both molecules is essentially that of a sawhorse structure in which the lone pair is apparently stereochemically active and occupies an equatorial position in a distorted trigonal bipyramid. The two methyl or phenyl groups occupy the other equatorial positions with Te−C bond lengths of 2.104(6) and 2.125(6) Å and a C−Te−C angle of 96.2(2)° in **2**. The corresponding values for **7** are 2.127(5) and 2.139(5) Å and 99.3(2)°. The axial positions are occupied by a sulfur atom from each of the dithiocarbonate groups to give anisobidentate linkages resulting in Te−S bonding distances of 2.590(2) and 2.677(2) Å, an S−Ge−S angle of 166.38(5)°, and S−Te−C angles ranging from 82.3(2) to 90.9(2)° in **2**. The corresponding distances and angles for **7** are 2.607(2) and 2.629(1) Å, 168.31(4)°, and a range from 83.0(1) to 90.4(1)°. There are also secondary intramolecular interactions involving both terminal sulfur atoms resulting in Te--S distances of 3.274(2) and 3.332(2) Å in **2** and 3.265(2) and 3.336(2) Å in **7**. These distances are discussed in terms of Pauling's partial bond orders, and if they are included as part of the coordination sphere, then the structure of **2** is better described as a pseudo pentagonal bipyramid with the supposed lone pair occupying an axial position, whereas the structure of **7** appears to be a distorted octahedron with an apparently inactive lone pair. The NMR spectra of the $Ph_2Te[S_2COR]_2$ series indicate that, for these five derivatives, reductive elimination is evident even in spectra recorded immediately following dissolution of the products.

Introduction

The continuing interest in tellurium complexes with sulfur ligands is exemplified by the recent comprehensive review by King *et al.* on stereochemical aspects and supramolecular associations.[1] Extensive studies have been carried out for a long time on *O*-alkyl dithiocarbonates (xanthates) as ligands, particularly on transition metals.[2] We report on xanthate derivatives of tellurium(IV) as an extension of our studies on related dithiocarbamates and dithiophosphates.[3−7] In general, the bonding between tellurium and sulfur has led to different interpretations of structural features because of the relatively large range of bond lengths attributed to Te−S bonding. Bonds considerably longer than the sum of the covalent radii have been invoked to account for dimeric associations in the di- and triorganotellurium(IV) xanthates $Me_2Te[S_2COMe]_2$[8] and $Ph_3Te[S_2COMe]$,[9] whereas $Ph_3Te[S_2CO(t\text{-}Bu)]$ is described as monomeric,[9] as was $C_8H_8Te[S_2COEt]_2$.[10] On the other hand, monoorganotellurium(II) xanthates of the type $[4\text{-}ROC_6H_4TeS_2COMe]_n$, where R = Me or Et, exist in double-strand polymeric chains[11,12] and $Te[S_2COEt]_2$ is described as a quasi dimer,[13,14] $Te[S_2CO(i\text{-}Pr)]_2$ as a monomer,[15] and Te[S$_2$COEt]Br as polymeric with bromine rather than sulfur bridges.[14] We report herein a systematic examination of two series of *O*-alkyl dithiocarbonate (xanthate) derivatives of dimethyl- and diphenyltellurium(IV), $Me_2Te[S_2COR]_2$ and $Ph_2Te[S_2COR]_2$, where R = Me, Et, *i*-Pr, *n*-Pr, and *n*-Bu, in an attempt to identify the

* Author to whom correspondence should be addressed.
† Current address: The Pulp and Paper Centre, University of Toronto, Toronto, Ontario, Canada M5S 1A4.
⊗ Abstract published in *Advance ACS Abstracts,* November 15, 1994.

(1) Haiduc, I.; King, R. B.; Newton, M. G. *Chem. Rev.* **1994**, *94*, 301.
(2) Burns, R. P.; McCullough, F. P.; McAuliffe, C. A. *Adv. Inorg. Chem. Radiochem.* **1980**, *23*, 211. Zeiss, W. C. *Acad. R. Sci. (Copenhagen)* **1815**, *1*, 1.
(3) Bailey, J. H. E.; Drake, J. E. *Can. J. Chem.* **1993**, *71*, 41.
(4) Bailey, J. H. E.; Drake, J. E.; Wong, M. L. Y. *Can. J. Chem.* **1991**, *69*, 1948.
(5) Bailey, J. H. E.; Drake, J. E.; Sarkar, A. B.; Wong, M. L. Y. *Can. J. Chem.* **1989**, *67*, 1735.
(6) Drake, J. E.; Wong, M. L. Y. *J. Organomet. Chem.* **1989**, *377*, 43.
(7) Chadha, R. K.; Drake, J. E.; McManus, N. T.; Quinlan, B. A.; Sarkar, A. B. *Organometallics* **1987**, *6*, 813.
(8) Wieber, M.; Schmidt, E; Burschka, C. *Z. Anorg. Allg. Chem.* **1985**, *525*, 127.
(9) Singh, A. K.; Basumatary, J. K.; Singh, T. P.; Padmanabhan, B. *J. Organomet. Chem.* **1992**, *424*, 33.
(10) Dakternieks, D.; Di Giacomo, R.; Gable, R. W.; Hoskins, B. F. *J. Am. Chem. Soc.* **1988**, *110*, 6753.
(11) Husebye, S.; Maartmann-Moe, K.; Mikalsen, O. *Acta Chem. Scand.* **1989**, *43*, 754.
(12) Hauge, S.; Vikane, O. *Acta Chem. Scand.* **1985**, *A39*, 553.
(13) Husebye, S. *Acta Chem. Scand.* **1967**, *21*, 42.
(14) Gable, R. W.; Hoskins, B. F.; Steen, R. J.; Winter, G. *Inorg. Chim. Acta* **1983**, *72*, 173.
(15) Hoskins, B. F.; Tiekink, E. R. T.; Winter, G. *Inorg. Chim. Acta* **1985**, *96*, L79.

0020-1669/95/1334-0124$09.00/0

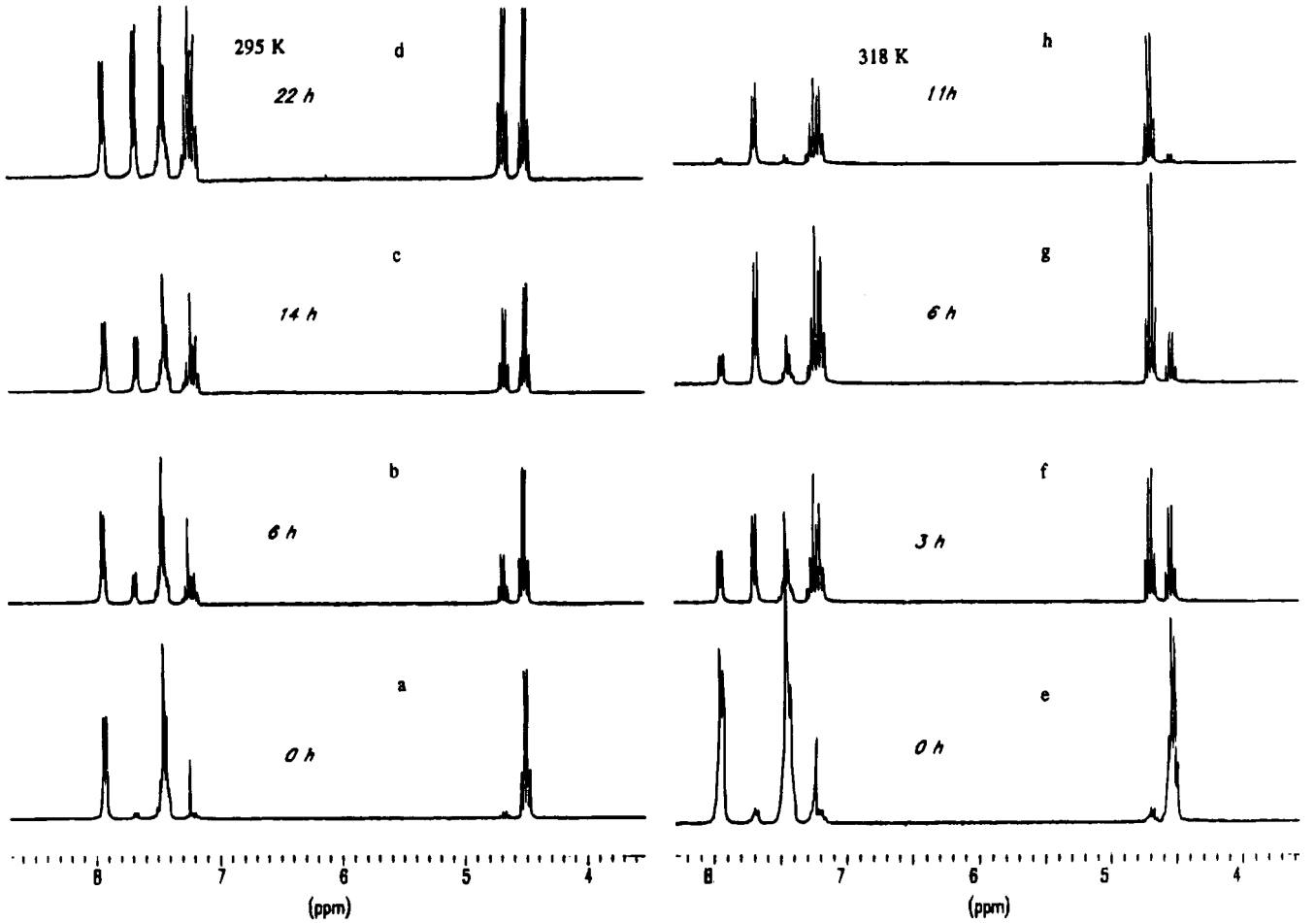

Figure 1. Portions of the ^{1}H NMR spectra of $Ph_2Te[S_2COEt]_2$ (**7**) recorded at 295 K (a−d) and 318 K (e−h) as part of the kinetic studies of its reductive elimination.

different effects of alkyl and aryl substitution on tellurium and of changing the nature of the alkyl group in the xanthate.

Experimental Section

Starting Materials. $TeCl_4$, Ph_4Sn, Me_4Sn, toluene, diethyl ether, petroleum ether, *n*-hexane, chloroform, and $CDCl_3$ were obtained from Aldrich. With the exception of toluene and chloroform, which were distilled, all materials were used as received. Carbon disulfide (BDH Chemicals) was distilled from P_4O_{10} prior to use.

Potassium *O*-alkyl dithiocarbonates were prepared by the addition of a slight excess of CS_2 to a mixture of equimolar amounts of KOH and ROH, where R = Me, Et, *i*-Pr, *n*-Pr, or *n*-Bu, in the manner described previously,[16] and their purities were checked by ^{1}H and ^{13}C NMR spectroscopy. All reactions were carried out on a vacuum line to exclude air and moisture by methods described previously.[17]

Ph_2TeCl_2 was prepared from an equimolar mixture of tetraphenyltin (4.5 g) and tellurium tetrachloride (2.87 g) in toluene (20 mL) by refluxing for 4 h at 60 °C and then working up the product in the manner described previously.[18] Me_2TeCl_2 was prepared by a procedure which was based on those previously reported for the preparation of Ph_2TeCl_2 from Ph_4Sn[18] and Ph_4Pb.[19] Tetramethyltin (2 mL) was added to a solution of tellurium tetrachloride (4 g) in toluene (25 mL). The flask was kept for 30 min at room temperature while the initial highly exothermic reaction took place. After 4 h of refluxing at 60 °C, a small amount of insoluble matter was removed by filtration. Petroleum ether was then added to the filtrate to bring about the precipitation of dimethyltellurium dichloride as a white powder. The product was filtered off, dried, and recrystallized from methanol or ethanol to give Me_2TeCl_2 (yield 65%; mp 92−94 °C).[20] Its purity was confirmed by its ^{1}H and ^{13}C NMR spectra.

Preparation of the $Me_2Te[S_2COR]_2$ Derivatives (1−5). $Me_2Te[S_2COEt]_2$ (2). Typically, dimethyltellurium dichloride (0.23 g, 1.0 mmol) was placed in a two-necked flask attached to the vacuum line. Previously dried potassium *O*-ethyl dithiocarbonate (0.39 g, 2.1 mmol) was introduced slowly from a finger-tube attached to the flask. After evacuation of the reaction vessel, chloroform or carbon disulfide (approximately 10 mL) was distilled in as the flask was held at −196 °C. The liquid nitrogen trap was then removed, and the contents were allowed to warm to ambient temperature with stirring, which was continued for 3−4 h at 0° C. The mixture was then filtered to remove unreacted KS_2COEt and KCl, and most of the solvent was pumped off to leave a solid residue, which was washed with *n*-hexane, dried under vacuum, and redissolved in CS_2, and the resultant solution was kept in a refrigerator. Narrow block-shaped crystals of $Me_2Te[S_2COEt]_2$ appeared after 2−3 days (0.28 g, 0.70 mmol, yield 70%; mp 78−79 °C). Anal. Calcd for $C_8H_{16}O_2S_4Te$: C, 24.02; H, 4.03. Found: C, 24.33; H, 4.06. Similarly was formed $Me_2Te[S_2COMe]_2$ (**1**) (needle shaped yellow crystals; yield 65%; mp 105−107 °C). Anal. Calcd for $C_6H_{12}O_2S_4Te$: C, 19.37; H, 3.35. Found: C, 19.44; H, 2.99. The same procedures when carried out for the other derivatives resulted in the formation of pale-yellow oils. These were redissolved in a few drops of *n*-hexane, which was then allowed to evaporate at room temperature, to give pale-yellow crystals. $Me_2Te[S_2CO(i\text{-}Pr)]_2$ (**3**): yield 65%; mp 65−67 °C. Anal. Calcd for $C_{10}H_{20}O_2S_4Te$: C, 28.06; H, 4.71. Found: C, 28.30; H, 4.55. $Me_2Te[S_2CO(n\text{-}Pr)]_2$ (**4**): yield 63%; mp 50−52 °C. Anal. Calcd for $C_{10}H_{20}O_2S_4Te$: C, 28.06; H,

(16) Vogel, A. I. *Practical Organic Chemistry*; Longmans: New York, 1956; p 499.
(17) Schmidt, M.; Schumann, H.; Gliniecki, F.; Jaggard, J. F. *J. Inorg. Nucl. Chem.* **1969**, *17*, 277.
(18) Paul, R. C.; Bhasin, K. K.; Chadha, R. K. *J. Inorg. Nucl. Chem.* **1975**, *37*, 2337.
(19) Pant, B. C. *J. Organomet. Chem.* **1973**, *54*, 191.
(20) Vernon, R. H. *J. Chem. Soc.* **1920**, *86*.

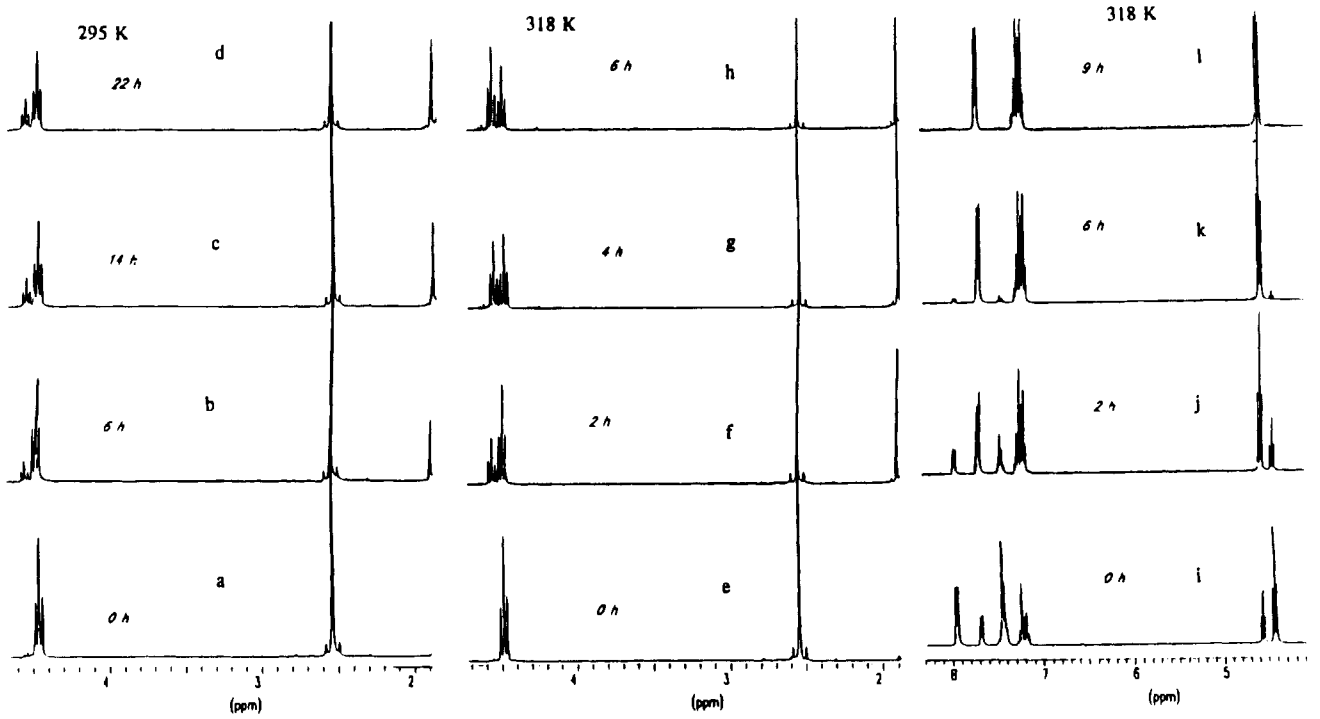

Figure 2. Portions of the ^{1}H NMR spectra of $Me_2Te[S_2CO(n\text{-}Pr)]_2$ (**4**) recorded at 295 K (a–d) and 318 K (e–h) and of $Ph_2Te[S_2CO(n\text{-}Pr)]_2$ (**7**) (i–l) recorded at 318 K as part of the kinetic studies of their reductive elimination.

4.71. Found: C, 28.02; H, 4.40. $Me_2Te[S_2CO(n\text{-}Bu)]_2$ (**5**): yield 60%; mp 46–48 °C. Anal. Calcd for $C_{10}H_{20}O_2S_4Te$: C, 31.59; H, 5.30. Found: C, 31.85; H, 5.22. Despite extensive efforts, it was only possible to obtain X-ray-quality crystals for **1**, **2**, and **7**.

Preparation of the $Ph_2Te[S_2COR]_2$ Derivatives (6–10). The preparations were carried out using the same procedures as for the $Me_2Te[S_2COR]_2$ series. Carbon disulfide was found to be a better solvent than chloroform. $Ph_2Te[S_2COMe]_2$ (**6**): pale-yellow crystals; yield 70%; mp 95–97 °C. $Ph_2Te[S_2COEt]_2$ (**7**): pale-yellow crystals; yield 67%; mp 116–117 °C. $Ph_2Te[S_2CO(i\text{-}Pr)]_2$ (**8**): bright-yellow crystals; yield 68%; mp 92–94 °C. Anal. Calcd for $C_{20}H_{24}O_2S_4Te$: C, 43.50; H, 4.38. Found: C, 43.10; H, 4.13. $Ph_2Te[S_2CO(n\text{-}Pr)]_2$ (**9**): pale-yellow crystals; yield 70%; mp 82–84 °C. $Ph_2Te[S_2CO(n\text{-}Bu)]_2$ (**10**): yellow oil, yield 65%.

Physical Measurements. The elemental analyses were performed by Guelph Chemical Laboratories, Guelph, Ontario, Canada. The ^{1}H and ^{13}C NMR spectra were recorded on a Bruker AC 300 FT NMR spectrometer in either CS_2 or $CDCl_3$ solution. The ^{125}Te NMR spectra were recorded on a Bruker AC 200 FT NMR spectrometer and referenced to dimethyltellurium. The infrared spectra were recorded on a Nicolet 5DX FT spectrometer as KBr or CsI pellets or as oils smeared between KBr windows in the 4000–400 cm^{-1} region. The far-infrared spectra were recorded on a Bomen DA3 infrared spectrometer between polyethylene plates as oils or as Nujol mulls. The Raman spectra were recorded on a JEOL-XY Raman spectrometer using the 5145-Å exciting line of an argon ion laser with samples sealed in capillary tubes. The melting points were determined on a Fisher-Johns apparatus.

For all compounds the NMR spectra were recorded immediately upon dissolving freshly prepared samples. Spectra of samples that had been stored as solids in the refrigerator or as solutions held at room temperature were also recorded. Kinetic runs were carried out on a cross section of products by recording the ^{1}H NMR spectra of $Me_2Te[S_2CO(n\text{-}Pr)]_2$ (**4**), $Me_2Te[S_2CO(n\text{-}Bu)_2$ (**5**), $Ph_2Te[S_2COEt]_2$ (**7**), and $Ph_2Te[S_2CO(n\text{-}Pr)]_2$ (**9**) in $CDCl_3$ solution using Me_4Si as internal standard. Samples of the spectra that were scanned every hour for 24 h at 295, 308, and 318 K are shown in Figures 1 and 2. Plots of ln-$[R'_2Te[S_2COR]_2]$ or ln[$ROCS_2S_2COR$] versus time were linear. Values of the first-order rate constants at 295 K (k_{295}), apparent activation energies (E_a), and Arrhenius preexponential factors (A) are as follows. $Me_2Te[S_2CO(n\text{-}Pr)]_2$ (**4**): k_{295}, 3.91 × 10^{-6} s^{-1}; E_a, 71 kJ mol^{-1}; A, 1.4 × 10^7 s^{-1}. $Me_2Te[S_2CO(n\text{-}Bu)]_2$ (**5**): k_{295}, 3.14 × 10^{-6} s^{-1}; E_a, 72 kJ mol^{-1}; A, 2.1 × 10^7 s^{-1}. $Ph_2Te[S_2COEt]_2$ (**7**): k_{295}, 8.40 × 10^{-6} s^{-1}; E_a, 57 kJ mol^{-1}; A, 8.6 × 10^4 s^{-1}. $Ph_2Te[S_2CO(n\text{-}Pr)]_2$ (**9**): k_{295}, 1.30 × 10^5 s^{-1}; E_a, kJ mol^{-1}; A, 5.3 × 10^5 s^{-1}.

Table 1. Crystallographic Data

	$Me_2Te[S_2COEt]_2$ (**2**)	$Ph_2Te[S_2COEt]_2$ (**7**)
chem formula	$C_8H_{16}O_2S_4Te$	$C_{18}H_{20}O_2S_4Te$
fw	400.05	524.19
a, Å	10.588(2)	11.320(3)
b, Å	11.974(2)	13.062(4)
c, Å	6.458(3)	8.225(4)
α, deg	104.06(3)	107.88(3)
β, deg	90.67(2)	110.72(3)
γ, deg	71.25(1)	79.91(3)
V, Å^3	750.2(8)	1078.3(8)
space group	$P\bar{1}$	$P\bar{1}$
Z	2	2
T, °C	23	23
λ, Å	0.710 69	0.710 69
ϱ_{calc}, g cm^{-3}	1.77	1.61
μ, cm^{-1}	25.04	17.80
transm factors	0.68–1.00	0.77–1.00
R^a	0.0310	0.0366
$R_w{}^b$	0.0286	0.0329

^{a} $R = \Sigma||F_o| - |F_c||/\Sigma|F_o|$. ^{b} $R_w = [(\Sigma w(|F_o| - |F_c|)^2/\Sigma wF_o^2)]^{1/2}$.

X-ray Crystallographic Analysis. Yellow block crystals of $Me_2Te[S_2COEt]_2$ (**2**) and $Ph_2Te[S_2COEt]_2$ (**7**) were sealed in thin-walled glass capillaries and mounted on a Rigaku AFC6S diffractometer, with graphite-monochromated Mo Kα radiation.

Cell constants and an orientation matrix for data collection, obtained from a least-squares refinement using the setting angles of 25 carefully centered reflections in the ranges $30.34 < 2\theta < 36.21°$ (for **2**) and $13.15 < 2\theta < 17.86°$ (for **7**), corresponded to triclinic cells whose dimensions are given in Table 1. On the basis of packing considerations, a statistical analysis of intensity distribution, and the successful solution and refinement of the structure, the space group was determined to be $P\bar{1}$ (No. 2) for both molecules.

The data were collected at a temperature of 23 ± 1 °C using the ω–2θ scan technique to a maximum 2θ values of 50.0°. The ω scans of several intense reflections, made prior to data collection, had average widths at half-height of 0.38° (for **2**) and 0.27° (for **7**) with a takeoff angle of 6.0°. Scans of $(1.57 + 0.30 \tan \theta)°$ (for **2**) and (1.42 + 0.30

tan θ)° (for **7**) were made at speeds of 32.0 and 16.0°/min (in ω) for **2** and **7**, respectively. The weak reflections ($I < 10.0\sigma(I)$) were rescanned (maximum of four rescans), and the counts were accumulated to ensure good counting statistics. Stationary-background counts were recorded on each side of the reflection. The ratio of peak counting time to background counting time was 2:1. The diameter of the incident-beam collimator was 0.5 mm, and the crystal to detector distance was 285.0 mm.

Of the 2809 (for **2**) and 4025 (for **7**) reflections which were collected, 2652 (for **2**) and 3813 (for **7**) were unique (R_{int} = 0.032 and 0.064 for **2** and **7**, respectively). The intensities of three representative reflections which were measured after every 150 reflections remained constant throughout data collection, indicating crystal and electronic stability (no decay correction was applied).

The linear absorption coefficients for Mo Kα were 25.0 cm^{-1} (for **2**) and 17.8 cm^{-1} (for **7**). An empirical absorption correction, based on azimuthal scans of several reflections, was applied, which resulted in transmission factors ranging from 0.68 to 1.00 (for **2**) and 0.77 to 1.00 (for **7**). The data were corrected for Lorentz and polarization effects.

The structure was solved by direct methods.[21] The non-hydrogen atoms were refined anisotropically, and the hydrogen atoms were included in their idealized positions with C−H set at 0.95 Å and with each isotropic thermal parameter set at 1.2 times that of the carbon atom to which it was attached. The final cycle of full-matrix least-squares refinement[22] was based on 1961 (for **2**) and 2939 (for **7**) observed reflections ($I > 3.00\sigma(I)$) and 136 (for **2**) and 226 (for **7**) variable parameters and converged (largest parameter shift was 0.001 times its esd) with weighted and unweighted agreement factors of $R = \sum||F_o| - |F_c||/\sum|F_o| = 0.0310$ (for **2**) and 0.0366 (for **7**) and $R_w = [\sum w(|F_o| - |F_c|)^2/\sum wF_o^2]^{1/2} = 0.0286$ (for **2**) and 0.0329 (for **7**).

The standard deviations of observations of unit weight[23] were 1.33 (for **2**) and 2.17 (for **7**). The weighting scheme was based on counting statistics and included a factor (p = 0.01 and 0.004 for **2** and **7**, respectively) to downweight the intense reflections. Plots of $\sum w(|F_o| - |F_c|)^2$ versus $|F_o|$, reflection order in data collection, (sin θ)/λ, and various classes of indices showed no unusual trends. The maximum and minimum peaks on the final difference Fourier maps corresponded to 0.50 and −0.56 e/Å^3, respectively, for **2** and 0.49 and −0.46, respectively, for **7**.

Neutral-atom scattering factors were taken from Cromer and Waber.[24] Anomalous dispersion effects were included in F_c,[25] the values for $\Delta f'$ and $\Delta f''$ were those of Cromer.[26] All calculations were performed using the TEXSAN[27] crystallographic software package of Molecular Structure Corp.

The final atomic coordinates and equivalent isotropic thermal parameters for the non-hydrogen atoms are given in Tables 2 and 3, important distances and bond angles in Tables 4 and 5, and ORTEP diagrams in Figures 3 and 4. Additional crystallographic data are available as supplementary material.

Data were also collected on crystal of $Me_2Te[S_2COMe]_2$ (**1**), and the solution was essentially identical to that reported earlier.[8]

(21) Structure solution methods: Calbrese, J. C. PHASE-Patterson Heavy Atom Solution Extractor. Ph.D. Thesis, University of Wisconsin—Madison, 1972. Beurskens, P. T. DIRDIF: Direct Methods for Difference Structures—an automatic procedure for phase extension and refinement of difference structure factors. Technical Report 1984/1; Crystallography Laboratory: Toernooiveld, 6525 Ed Nijmegen, The Netherlands, 1984.

(22) Least-squares: function minimized: $\sum w(|F_o| - |F_c|)^2$, where $w = 4F_o^2\sigma(F_o^2)$, $\sigma^2(F_o^2) = [S^2(C + R^2B) + (pF_o^2)^2]/(Lp)^2$, S = scan rate, C = total integrated peak count, R = ratio of scan time to background counting time = B, Lp = Lorentz−polarization factor, and $p = p$ factor.

(23) Standard deivation of an observation of unit weight: $[\sum w(|F_o| - |F_c|)^2/(N_o - N_v)]^{1/2}$, where N_o = number of observations and N_v = number of variables.

(24) Cromer, D. T.; Waber, J. T. *International Tables for X-ray Crystallography*; The Kynoch Press: Birmingham, England, 1974; Vol. IV, Table 2.2 A.

(25) Ibers, J. A.; Hamilton, W. C. *Acta Crystallogr.* **1964**, *17*, 781.

(26) Cromer, D. T. *International Tables for X-ray Crystallography*; The Kynoch Press: Birmingham, England, 1974; Vol. IV, Table 2.3.1.

(27) *TEXSAN-TEXRAY Structure Analysis Package*; Molecular Structure Corp.: Woodlands, TX, 1985.

Table 2. Final Fractional Coordinates and B(eq) Values for Non-Hydrogen Atoms of $Me_2Te[S_2COEt]_2$ (**2**) with Standard Deviations in Parentheses

atom	x	y	z	B(eq), Å^2
Te(1)	0.05938(4)	0.27149(4)	0.51163(6)	2.78(2)
S(1)	−0.1530(1)	0.4740(1)	0.6353(2)	3.65(8)
S(2)	−0.1896(2)	0.3376(1)	0.1943(2)	4.3(1)
S(3)	0.2749(2)	0.0871(2)	0.4874(2)	4.4(1)
S(4)	0.1416(2)	0.0488(2)	0.0754(3)	4.5(1)
O(1)	−0.3488(4)	0.5497(3)	0.4254(6)	3.9(2)
O(2)	0.3930(4)	−0.0605(3)	0.1442(6)	3.7(2)
C(1)	−0.0573(6)	0.1746(5)	0.597(1)	3.9(3)
C(2)	0.1139(6)	0.3343(6)	0.825(1)	4.1(4)
C(3)	−0.2376(5)	0.4551(5)	0.4041(9)	2.9(3)
C(4)	−0.4396(6)	0.5513(6)	0.252(1)	4.4(4)
C(5)	−0.5538(6)	0.6699(6)	0.319(1)	4.8(4)
C(6)	0.2724(6)	0.0198(5)	0.2181(9)	3.4(3)
C(7)	0.4165(6)	−0.1258(6)	−0.082(1)	4.4(4)
C(8)	0.5548(6)	−0.2145(5)	−0.111(1)	4.6(4)

Table 3. Final Fractional Coordinates and B(eq) Values for Non-Hydrogen Atoms of $Ph_2Te[S_2COEt]_2$ (**7**) with Standard Deviations in Parentheses

atom	x	y	z	B(eq), Å^2
Te(1)	0.35562(4)	0.73017(3)	0.48682(5)	2.68(1)
S(1)	0.4580(2)	0.7375(1)	0.2527(2)	3.93(7)
S(2)	0.5880(2)	0.5522(1)	0.4133(2)	4.50(7)
S(3)	0.2531(1)	0.7657(1)	0.7425(2)	3.23(6)
S(4)	0.0704(2)	0.6501(1)	0.3938(2)	4.83(8)
O(1)	0.6217(4)	0.6021(3)	0.1462(5)	4.1(2)
O(2)	0.0503(4)	0.7036(3)	0.7196(5)	4.4(2)
C(1)	0.5023(5)	0.8164(4)	0.6997(7)	2.9(2)
C(2)	0.5542(6)	0.7851(4)	0.8591(8)	3.5(2)
C(3)	0.6478(6)	0.8415(6)	0.9983(8)	4.8(3)
C(4)	0.6911(6)	0.9278(6)	0.9824(9)	5.0(3)
C(5)	0.6382(7)	0.9611(5)	0.823(1)	5.5(3)
C(6)	0.5451(6)	0.9057(5)	0.6829(8)	4.3(3)
C(7)	0.2337(5)	0.8632(4)	0.4019(7)	2.9(2)
C(8)	0.2270(6)	0.9641(4)	0.5203(8)	4.3(3)
C(9)	0.1370(7)	1.0448(5)	0.459(1)	5.5(3)
C(10)	0.0572(7)	1.0229(5)	0.290(1)	5.3(3)
C(11)	0.0661(6)	0.9233(5)	0.1721(9)	4.7(3)
C(12)	0.1518(6)	0.8432(4)	0.2269(8)	3.7(2)
C(13)	0.5618(5)	0.6229(4)	0.2682(7)	3.2(2)
C(14)	0.7127(6)	0.5049(5)	0.1307(8)	4.5(3)
C(15)	0.7676(7)	0.5081(5)	−0.007(1)	5.7(3)
C(16)	0.1155(5)	0.7024(4)	0.6148(8)	3.3(2)
C(17)	−0.0711(6)	0.6588(5)	0.646(1)	5.5(3)
C(18)	−0.1218(8)	0.6757(7)	0.793(1)	8.4(5)

Calculation of Pauling Bond Order. The formula proposed by Pauling[28] for partial bonds is given by $d_n - d = -0.60 \log n$, where d_n is the bond length for bond number n and d is the length of the single bond of the same type. On the basis of the C−C single bond of 1.54 Å, Pauling's formula gives bond lengths of 1.36 Å for n = 2, 1.72 Å for n = 0.5, and 1.90 Å for n = 0.25. These give increases in bond length for the partial bonds of approximately 12 and 23% respectively for n = 0.5 and 0.25. It is reasonable to assume that similar expressions relating bond order to interatomic distances for the much longer secondary interactions or partial bonds involving Te and S should utilize percentage differences "normalized" to 1.54 rather than absolute differences. Pauling's relationship, which can be written as $n = 10^X$, where $X = (d - d_n)/0.6$, can be modified to allow for percentage differences "normalized" to 1.54 so that now $X = [1.54(d - d_n)/d]/0.6$ or $X = 2.5(d - d_n)/d$. On the basis of a Te−S single bond length of 2.63 Å, typical calculated values of the lengths of partial bonds for various values of n are as follows: 2.63 Å (n = 1.0), 2.76 (0.75), 2.95 (0.50, 3.26 (0.25), 3.68 (0.10). This scale appears to be compatible with the sum of the van der Waals radii of 3.86 Å for Te and S.[29]

(28) Pauling. L. *J. Am. Chem. Soc.* **1947**, *69*, 542. Pauling, L. *The Nature of the Chemical Bond*, 3rd ed.; Cornell University Press: Ithaca, NY, 1960; p 255.

(29) Bondi, A. *J. Phys. Chem.* **1964**, *68*, 441.

Table 4. Important Interatomic Distances (Å) and Angles (deg) for $Me_2Te[S_2COEt]_2$ (**2**)[a,b]

Te(1)–C(1)	2.104(6)	Te(1)–C(2)	2.125(6)
Te(1)–S(1)	2.677(2)	Te(1)–S(3)	2.590(2)
S(1)–C(3)	1.737(5)	S(3)–C(6)	1.734(6)
S(2)–C(3)	1.645(5)	S(4)–C(6)	1.645(6)
O(1)–C(3)	1.326(6)	O(2)–C(6)	1.336(6)
O(1)–C(4)	1.468(6)	O(2)–C(7)	1.460(6)
C(4)–C(5)	1.509(8)	C(7)–C(8)	1.489(8)
Te(1)–S(2)	3.331(2)	Te(1)–S(4)	3.274(2)
Te(1)- -S(1)′	3.814(2)		
Te(1)- -S(2)″	4.925(6)	Te(1)- -S(4)″	4.927(8)
S(1)–Te(1)–S(3)	166.39(5)	C(1)–Te(1)–C(2)	96.2(2)
S(1)–Te(1)–C(1)	87.9(2)	S(3)–Te(1)–C(1)	90.9(2)
S(1)–Te(1)–C(2)	82.3(2)	S(3)–Te(1)–C(2)	84.3(2)
S(1)–Te(1)–S(2)	58.90(5)	S(3)–Te(1)–S(4)	60.28(5)
S(2)–Te(1)–S(4)	74.04(5)		
Te(1)–S(1)–C(3)	97.8(2)	Te(1)–S(3)–C(6)	96.4(3)
S(1)–C(3)–S(2)	125.6(3)	S(3)–C(6)–S(4)	125.4(3)
S(1)–C(3)–O(1)	109.1(4)	S(3)–C(6)–O(2)	109.6(4)
S(2)–C(3)–O(1)	125.3(4)	S(4)–C(6)–O(2)	125.0(4)
C(3)–O(1)–C(4)	118.7(4)	C(6)–O(2)–C(7)	119.5(4)
O(1)–C(4)–C(5)	106.6(5)	O(2)–C(7)–C(8)	106.8(5)

[a] Symmetry-equivalent position ($-x$, $1-y$, $1-z$) is denoted by a prime and (x, y, $1+z$) by a double prime. [b] Numbers in parentheses refer to estimated standard deviations in the least significant digits.

Table 5. Important Interatomic Distances (Å) and Angles (deg) for $Ph_2Te[S_2COEt]_2$ (**7**)[a,b]

Te(1)–C(1)	2.127(5)	Te(1)–C(7)	2.139(5)
Te(1)–S(1)	2.607(2)	Te(1)–S(3)	2.629(1)
S(1)–C(13)	1.729(5)	S(3)–C(16)	1.733(6)
S(2)–C(13)	1.639(5)	S(4)–C(16)	1.657(6)
O(1)–C(13)	1.337(6)	O(2)–C(16)	1.314(6)
O(1)–C(14)	1.480(6)	O(2)–C(17)	1.447(7)
C(14)–C(15)	1.485(8)	C(17)–C(18)	1.453(8)
Te(1)–S(2)	3.265(2)	Te(1)–S(4)	3.336(2)
ring C(1)–C(6) mean C–C	1.39(2)	ring C(7)–C(12) mean C–C	1.37(2)
S(1)–Te(1)–S(3)	168.31(4)	C(1)–Te(1)–C(7)	99.3(2)
S(1)–Te(1)–C(1)	90.4(1)	S(3)–Te(1)–C(1)	83.0(1)
S(1)–Te(1)–C(7)	83.2(1)	S(3)–Te(1)–C(7)	88.4(1)
S(1)–Te(1)–S(2)	60.30(4)	S(3)–Te(1)–S(4)	59.35(5)
S(2)–Te(1)–S(4)	119.89(5)		
Te(1)–S(1)–C(13)	96.7(2)	Te(1)–S(3)–C(16)	98.5(2)
S(1)–C(13)–S(2)	126.2(3)	S(3)–C(16)–S(4)	125.7(3)
S(1)–C(13)–O(1)	109.2(3)	S(3)–C(16)–O(2)	109.7(4)
S(2)–C(13)–O(1)	124.6(4)	S(4)–C(16)–O(2)	124.7(5)
C(13)–O(1)–C(14)	118.7(4)	C(16)–O(2)–C(17)	121.1(5)
O(1)–C(14)–C(15)	105.6(5)	O(2)–C(17)–C(18)	108.3(6)
Te(1)–C(1)–C(2)	119.2(4)	Te(1)–C(7)–C(8)	122.0(6)
Te(1)–C(1)–C(6)	121.1(4)	Te(1)–C(7)–C(12)	117.7(4)
ring C(1)–C(6) mean C–C–C	120.0(6)	ring C(7)–C(12) mean C–C–C	120.0(7)

[a] Symmetry-equivalent position ($-x$, $1-y$, $1-z$) is denoted by a prime and (x, y, $1+z$) by a double prime. [b] Numbers in parentheses refer to estimated standard deviations in the least significant digits.

Results and Discussion

Various *O*-alkyl dithiocarbonate derivatives of dimethyl- and diphenyltellurium(IV) can be prepared by the addition of a slight excess of the potassium salt of the appropriate dithiocarbonic acid with dimethyl- or diphenyltellurium dichloride in carbon disulfide or chloroform as solvent in accord with the general equation

$$R'_2TeCl_2 + 2KS_2COR \rightarrow R'_2Te[S_2COR]_2 + 2KCl$$

$$R' = Me, Ph; R = Me, Et, i\text{-}Pr, n\text{-}Pr, n\text{-}Bu$$

All of these $Me_2Te[S_2COR]_2$ and $Ph_2Te[S_2COR]_2$ derivatives, with the exception of $Ph_2Te[S_2CO(n\text{-}Bu)]_2$, which is obtained as a yellow paste that changes to an oil as it is warmed to room temperature, can be isolated as solids, which are sufficiently stable to provide sharp melting points and NMR spectra of the pure compounds. All of the compounds undergo reductive elimination in accord with the equation

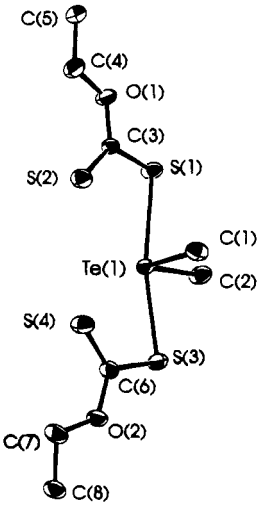

Figure 3. ORTEP plot of the molecule $Me_2Te[S_2COEt]_2$ (**2**). The atoms are drawn with 30% probability ellipsoids, and hydrogen atoms are omitted for clarity.

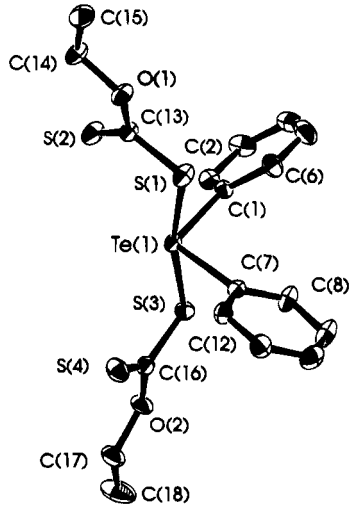

Figure 4. ORTEP plot of the molecule $Ph_2Te[S_2COEt]_2$ (**7**). The atoms are drawn with 30% probability ellipsoids, and hydrogen atoms are omitted for clarity.

$$R'_2Te[S_2COR]_2 \rightarrow R'_2Te + ROCS_2S_2COR$$

The process takes place rapidly for the diphenyltellurium derivatives (**6**–**10**), which are unstable even as solids at room temperature and in solution are 50% decomposed in a matter of 12–24 h. By contrast, sealed solid samples of the dimethyltellurium derivatives (**1**–**5**) are essentially stable indefinitely at room temperature, show negligible signs of decomposition when their spectra are recorded immediately on dissolution, and require from 2 to 4 days to reach 50% decomposition.

Kinetic studies carried out on a cross section of the derivatives, namely on **4**, **5**, **7** and **9**, indicate that the reaction is first order with energies of activation of approximately 71 and 58 kJ mol^{-1}, respectively, for the reductive elimination of the $Me_2Te[S_2COR]_2$ and $Ph_2Te[S_2COR]_2$ compounds. The nature of the organic group in the xanthate appears to have little effect whereas there is a significant difference between the reactions

leading to Me_2Te and those leading to Ph_2Te. The differences in the rates of reductive elimination are well illustrated by Figures 1 and 2. The portions of the ^1H NMR spectra of $Ph_2Te[S_2COEt]_2$ (**7**) shown in Figure 1 contrast the rate of reductive elimination at room temperature (a–d) and 318 K (e–h). In Figure 1a the peaks attributable to the phenyl groups of **7** are clearly seen centered at 7.90 and 7.45 ppm as is the quartet centered at 4.46 ppm assignable to the CH_2 protons of the OEt group in **7**. Peaks assignable to Ph_2Te and the diligand are barely discernible in Figure 1a, but after 22 h at room temperature, Figure 1d clearly shows the peaks assignable to Ph_2Te at 7.64 and 7.23 ppm and those of the CH_2 protons in $CH_3CH_2COS_2S_2COCH_2CH_3$ at 4.66 ppm of about the same intensity as those of **7**. By contrast, after only 11 h at 318 K (Figure 1h), the peaks attributable to $Ph_2Te[S_2COEt]_2$ (**7**) have virtually disappeared. Figure 2 presents portions of the spectra of $Me_2Te[S_2CO(n\text{-}Pr)]_2$ (**4**) run at room temperature (a–d) and 318 K (e–h) along with those of $Ph_2Te[S_2CO(n\text{-}Pr)]_2$ (**9**) run at 318 K (i–l). The initial spectra, Figure 2a,e, show the triplet of the OCH_2 protons and the singlet of the $(CH_3)Te$ protons in **4** at 4.45 and 2.53 ppm, respectively. Even after 22 h at room temperature, the peaks attributable to the OCH_2 protons of $CH_3CH_2CH_2OCS_2S_2COCH_2CH_2CH_3$ at 4.55 ppm and that attributable to $(CH_3)_2Te$ at 1.72 ppm are of relatively low intensity. A comparison with the spectra of $Ph_2Te[S_2CO(n\text{-}Pr)_2]_2$ (**9**) at 318 K shows that after 6 h (Figure 2k) the reductive elimination of **9** is nearly complete, whereas for $Me_2Te[S_2CO(n\text{-}Pr)]_2$ (**4**), integration of the peaks indicates that it has proceeded approximately 51% toward completion (Figure 2h). It should also be noted that the two dimethyltellurium derivatives, $Me_2Te[S_2CO(n\text{-}Pr)]_2$ and $Me_2Te[S_2CO(n\text{-}Bu)]_2$, have energies of activation of 71 and 72 kJ mol^{-1}, respectively, while those of the diphenyl derivatives, $Ph_2Te[S_2COEt]_2$ and $Ph_2Te[S_2CO(n\text{-}Pr)]_2$, are 57 and 59 kJ mol^{-1}, respectively, emphasizing the dependence of reductive elimination on the nature of the organic group on tellurium rather than those in the xanthate.

Molecular Structure of $Me_2Te[S_2COEt]_2$ (2). Dimethyl- and diphenylbis(*O*-ethyl dithiocarbonato)tellurium(IV) (**2** and **7**) both crystallize in the space group $P\bar{1}$. The ORTEP diagrams (Figures 3 and 4) illustrate that the immediate environment about tellurium in both **2** and **7** can be described as the sawhorse structure typical of tellurium(IV) compounds in which the lone pair is apparently stereochemically active and occupies an equatorial position in a distorted trigonal bipyramid. The supposed lone pair is located approximately in the position of the Te(1) label, and the two methyl or phenyl groups occupy the other two equatorial positions with the axial positions being occupied by a sulfur atom from each of the dithiocarbonate groups. The Te–C(methyl) and Te–C(phenyl) bond lengths of 2.104(6) and 2.125(6) Å in **2** and 2.127(5) and 2.139(5) Å in **7** are similar to those reported for the 1,3-dihydro-2λ^4-benzotellurole-2,2-diyl bis(*O*-ethyl xanthate), $C_8H_8Te[S_2COEt]_2$,[10] and for $Me_2Te[S_2COMe]_2$, which also crystallized in the space group $P\bar{1}$,[8] and slightly shorter than found in $Me_2Te[S_2CNMe_2]_2$.[3] The Te–C(methyl) bond lengths in **2** are essentially the same as the mean of Te–C(aromatic) bonds (2.116 Å) and shorter than the mean of Te–C(aliphatic) bonds (2.158 Å).[30] The same phenomenon was noted in a comparison of the structure of $Me_2Te[S_2CNMe_2]_2$ to that of its $Ph_2Te[S_2NR_2]_2$ analogues[3] and suggests a relatively stronger Te–C(methyl) bond than might be anticipated in view of the fact that Te–C(aromatic) bonds are generally stronger than Te–C(aliphatic)

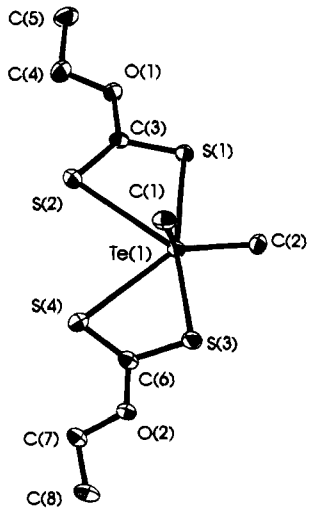

Figure 5. ORTEP plot of the molecule $Me_2Te_2[S_2COEt]_2$ (**2**) showing the inclusion of intramolecular Te--S interactions as part of the coordination sphere resulting in the formation of a pentagonal plane. The atoms are drawn with 30% probability ellipsoids, and hydrogen atoms are omitted for clarity.

bonds. The Te–S bond distances in $Me_2Te[S_2COEt]_2$ (**2**) of 2.590(2) and 2.677(2) Å bracket those of $C_8H_8Te[S_2COEt]_2$, which average 2.63(1) Å. The longer Te–S bond is associated with S(1), which is the only sulfur atom with an intermolecular contact under 5.0 Å in **2** at 3.814(2) Å. In $Me_2Te[S_2COMe]_2$, the corresponding sulfur atom is 3.755(1) Å from an adjacent tellurium atom, which is the only such contact less than the sum of the van der Waals radii of approximately 3.9 Å.[29] A similar phenomenon was noted for R_2TeCl_2, where one Te–Cl bond was much longer than the other and it too appeared to be the only one involved in any intermolecular association.[31] The nature of these interactions is not clear, but as was proposed recently in discussing an unusually long Si–Si bond,[32] we have made estimates of the Pauling bond order,[28] which suggest that the intermolecular interaction of 3.814(2) Å approximates to a bond order of only 0.07. This may indicate that the difference in the Te–S bond lengths is more a matter of packing than of a secondary interaction. However, in $Ph_2Te[S_2COEt]_2$ (**7**) there are no secondary interactions involving the Te-bonded sulfur atoms less than the sum of the van der Waals radii, and the two Te–S bond lengths are 2.607(2) and 2.629(1) Å.

The intramolecular Te--S interactions, which average 3.30(4) Å in **2** and **7**, correspond to an approximate bond order of 0.23, which suggests that these can be described as anisobidentate ligands and that these secondary interactions should be included in the coordinating sphere. This was the view of the authors reporting the structure of $Me_2Te[S_2COMe]_2$[8] because they describe the structure as a pesudo pentagonal bipyramid rather than a pseudo trigonal bipyramid. The projection of **2** in Figure 5 demonstrates a similar arrangement in which S(1), S(2), S(3), S(4), and C(2) form an approximate pentagonal plane (mean deviation from plane is 0.027 Å), with Te(1) only just out of the plane (0.07(1) Å) and with C(1) taking up one axial position (2.01(1) Å above the plane) and the supposed lone pair the other position below the plane. The dihedral angle between the plane Te(1), S(1), and S(2) and the plane Te(1), S(3), and

(30) Allen, F. H.; Kennard, O.; Watson, D. G.; Brammer, L.; Orpen, A. G.; Taylor R. *J. Chem. Soc., Perkin Trans. 2* **1987**, S1.

(31) Chadha, R. J.; Drake, J. E.; Hencher, J. L. *Can. J. Chem.* **1983**, *61*, 1222.

(32) Boch, H.; Ruppert, K.; Nather, C.; Havlas, Z.; Herrmann, H.-F.; Arad, C.; Gobel, I.; John, A.; Meuret, J.; Nick, S.; Rauschenbach, A.; Seitz, W.; Vaupel, T.; Solouki, B. *Angew. Chem., Int. Ed. Engl.* **1992**, *31*, 550.

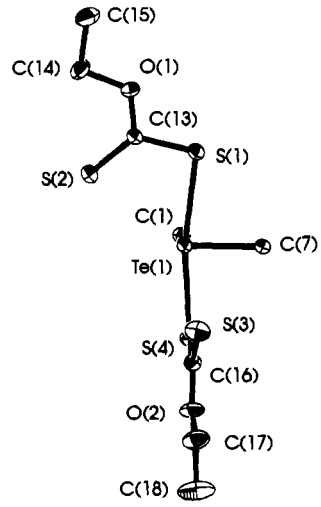

Figure 6. ORTEP plot of the molecule $Ph_2Te[S_2COEt]_2$ (**7**) demonstrating the orientaiton of the two dithiocarbonic groups. The atoms are drawn with 30% probability ellipsoids, and hydrogen atoms and carbon atoms of the phenyl rings that are not attached to tellurium are omitted for clarity.

S(4) is 176.0(1)°. By contrast, when the anisobidentate sulfur atoms are considered to be part of the coordination sphere in **7**, the environment about tellurium is a distorted octahedron with the anisobonded sulfur atoms taking up positions approximately cis and trans to the two phenyl groups. The projection of **7** in Figure 6, demonstrates that one of the phenyl carbon atoms attached to tellurium, C(1), Te(1), S(3), and S(4) are essentially coplanar (mean deviation from plane is 0.026 Å) with the second phenyl carbon atom C(7) out of the plane by 2.11(1) Å, along with S(2). Similarly C(7), Te(1), S(1), and S(2) are approximately coplanar (mean deviation of 0.023 Å) with C(1) out of plane by 2.09(1) Å, along with S(4). The dihedral angle between the plane Te(1), S(1), and S(2) and the plane Te(1), S(3), and S(4) is 80.4(1)°, indicating the marked difference of the orientation of the two groups in **7** and **2** and the relatively little distortion from the arrangement that would exist if the linakges were bidentate with the anisobonded atoms cis to one another. This distorted octahedral arrangement about tellurium implies an inactive lone pair. The structure of $C_8H_8Te[S_2COEt]_2$[10] is described as an eight-coordinate dimer because, in addition to the two Te−S intramolecular contacts at approximately 3.30 Å, there is an intermolecular contact at 3.4796(7) Å that has no counterpart in **2** or **7** or their methyl xanthate analogues. It was suggested that dithiocarbamates have stronger chelating ability than xanthates because the secondary Te−S bonds in $C_8H_8Te[S_2CNEt_2]_2$ were slightly shorter than those of the correpsonding xanthate. The Te−S secondary interactions in **2** and **7** are slightly longer than those in the two forms of the corresponding dithiocarbamate, $Ph_2Te[S_2CNEt_2]_2$.[31]

The closing of the S−Te−S angle from 180 to 166.39(5)° in **2** and to 168.31(4)° in **7** is essentially the same as reported for the C_8H_8 analogue. It is also similar in $Me_2Te[S_2COMe]_2$[8] and $Me_2Te[S_2CNMe_2]_2$,[3] where the angles are 165.90(3) and 166.5(1)°, respectively. These angles are smaller than any reported previously for similar diphenyl derivatives where values range from 172.0(1)° in $Ph_2Te[S_2CNMe_2]_2$[5] to 178.94(2)° in the *C2/c* form of Ph_2 $Te[S_2CNEt_2]_2$.[33] No obvious trends are evident for the C−Te−C bond angles. The angle of 96.2(2)° in **2** is essentially the same as that in $Me_2Te[S_2COMe]_2$ and is larger than the values of 93.9(2) and 95.5(3)° reported for $Me_2Te[S_2CNMe_2]_2$. The angle of 99.3(2)° in **7** is the same as the value of 99.4(1)° in $Ph_2Te[S_2CNMe_2]_2$ but much larger than that of 92.6(4)° in $(p\text{-}MeOC_6H_4)_2Te[S_2CNMe_2]_2$.[5] The bite angles in **2** and **7** range from 58.90(5) to 60.30(4)°, which are comparable to those of 59.08(2) and 59.80(2)° reported for $C_8H_8Te[S_2COEt]_2$[10] and very much less than would be the case for a truly bidentate ligand where a typical value is approximately 69°.

The terminal or anisobidentate C=S bonds in **2** and **7** are considerably shorter (1.645(6) Å in **2**, 1.639(5) and 1.657(6) Å in **7**) than the TeS−C bonds (1.734(6) and 1.737(5) Å in **2**, 1.729(5) and 1.733(6) Å in **7**). These bond lengths are essentially the same as those reported for $C_8H_8Te[S_2COEt]_2$.[10] The distortion of the angles around the planar thio-carbon atom is also essentially the same in **2**, **7**, the C_8H_8 derivative, and $Me_2Te[S_2COMe]_2$.[8] In **2** and **7** the S=C−S and S=C−O angles, which average 125.7(4) and 124.9(3)°, respectively, are not only similar but also considerably larger than the average value of 109.4(3)° for the (Te)S−C−O angle, suggesting similar π-bond character in the bonds involving the terminal sulfur and oxygen atoms and very little if any in the (Te)S−C bonds. The S_2C-O bond is certainly appreciably shorter (an average of 1.33(1) Å in **2** and **7**) compared to the $O-CH_2$ bond (an average of 1.46(1) Å).

Infrared and Raman Spectra. Distinctive features in the infrared and Raman spectra and their assignments are given in Table 6 for compounds **1**−**5** and in Table 7 for **6**−**10**. The spectra of dithiocarbonate derivatives, whether it be salts or metal complexes, typically show three very intense peaks within the range 1250−1020 cm^{-1} assignable to S_2COC stretching vibrations. These dominate the spectra relative to the peaks assignable to phenyl or alkyl groups.[34,35] The intensity reflects the large changes in dipole moment resulting from contributions from C−O stretching in all three vibrations. Conversely, while these three vibrations are very weak or not observed in the Raman spectra, the fourth S_2COC stretching vibration, $\nu(S_2COC)_d$, predominantly involves the symmetric CS_2 vibration and so is typically observed as a relatively intense peak in the region 690−640 cm^{-1}. The assignments in Tables 6 and 7 make use of such factors as three peaks of similar relative intensity at close to 728, 680, and 450 cm^{-1} that are consistent features in the infrared spectra of Ph_2TeX_2 compounds, where they are the most intense features associated with the phenyl groups attached to tellurium; the peak close to 1000 cm^{-1} in the Raman spectra, which is consistently the most intense feature of the phenyl groups; the distincitve infrared peak attributable to one of the methyl rocking modes at 800−808 cm^{-1} for the group attached to tellurium; comparisons with the spectra of the starting salts, KS_2COR; and the most recent of attempts at the vibrational analyses of alkyl xanthates.[36]

In compounds **1**−**5**, the asymmetric and symmetric CH_3−Te stretches are assigned to peaks in the region 535−525 cm^{-1}. These features are weak in the infrared spectra but strong in the Raman spectra relative to those of the thio ligand. The values are similar for all five derivatives and almost identical to those for Me_2TeI_2,[37] and the near coincidence of these modes is consistent with a C−Te−C angle close to 90°. The next two prominent peaks in the Raman spectra, which are not related to features in the salts, are assigned to the asymmetric and

(33) Dakternicks, D.; DiGiacomo, R.; Gable, R. W.; Hoskins, B. F. *J. Organomet. Chem.* **1988**, *349*, 305.

(34) Drake, J. E.; Mislankar, A. G.; Wong, M. L. Y. *Inorg. Chem.* **1991**, *30*, 2174.

(35) Drake, J. E.; Mislankar, A. G.; Yang, J. *Inorg. Chim. Acta* **1993**, *211*, 37.

(36) Colthup, N. B.; Powell, L. P. *Spectrochim. Acta* **1987**, *43A*, 317.

(37) Hayward, G. C.; Hendra, P. J. *J. Chem. Soc. A* **1969**, 1760.

Table 6. Selected Features (cm^{-1}) and Their Assignments in the Vibrational Spectra of Compounds **1**–**5**[a,b]

$Me_2Te[S_2COMe]_2$ (**1**)		$Me_2Te[S_2COEt]_2$ (**2**)		$Me_2Te[S_2CO(i\text{-}Pr)]_2$ (**3**)		$Me_2Te[S_2CO(n\text{-}Pr)]_2$ (**4**)		$Me_2Te[S_2CO(n\text{-}Bu)]_2$ (**5**)		
IR[c]	Raman[d]	IR[c]	Raman[d]	IR[c]	Raman[d]	IR[c]	Raman[d]	IR[c]	Raman[d]	assgnt
1204 vs	*f*	1179 s	*f*	1200 vs	*f*	1194 vs	*f*	1180 s, br	*f*	$\nu(S_2COC)_a$[e]
1143 s	*f*	1104 s	*f*	1084 vs	*f*	1133 m	*f*	1124 s	*f*	$\nu(S_2COC)_b$[e]
1047 vs	1052 (30)	1033 vs	1042 (20)	1021 vs	1018 (5)	1046 vs	1041 (15)	1037 vs, br	1038 (30)	$\varrho(S_2COC)_c$[e]
803 m	*f*	806 m	*f*	801 ms	801 (15)	804 ms	*f*	808 ms	*f*	$\varrho(CH_3Te)$
629 vw.	631 (50)	668 w	674 (30)	663 mw	673 (15)	668 w	669 (30)	670 m	667 (50)	$\nu(S_2COC)_d$[e]
527 w, br	536 (35)	526 vw, br	535 (75)	538 vw	536 (60)	528 w, br	538 (80)	520 mw, br	535 (65)	$\nu(Te-C)_{asym}$
527 w, br	522 (60)	526 vw, br	526 (100)	515 w	517 (60)	528 w, br	531 (100)	520 mw, br	521 (100)	$\nu(Te-C)_{sym}$
461 m	458 (5)	440 m	440 (5)	456 m	454 (10)	433 m	435 (5)	436 m	423 (25)	δ(COC)
368 ms	368 (90)	363 mw	382 (45)	390 mw	393 (60)	360 ms	364 (20)	374 m	378 (80)	$\nu(Te-S)_{asym}$
279 w	279 (20)	312 s	301 (55)	292 s	312 (100)	313 ms	315 (35)	290 ms	304 (65)	$\nu(Te-S)_{sym}$
199 s	201 (100)	211 m	213 (65)	210 s	215 (80)	204 m	204 (45)	212 mw	219 (60)	δ(CTeC)

[a] Parentheses denote relative intensities in the Raman effect. [b] s = strong, m = medium, w = weak, sh = shoulder, br = broad, and v = very. [c] Run neat between KBr plates down to 400 cm^{-1} and between polyethylene below 400 cm^{-1}. [d] Run neat in sealed capillaries. [e] In the xanthate salts, KS_2COR, these appear for R = Me at 1187 s, 1109 vs, 1049 vs, 620 (100), 476 (30); for R = Et at 1143 s, 1105 vs, 1050 s, 666 (100), 448 (55); for R = *i*-Pr at 1135 s, 1084 vs, 1056 vs, 660 (100), 462 (60); for R = *n*-Pr at 1150 s, 1117 vs, 1068 s, 659 (100), 454 (70); and for R = *n*-Bu at 1147 s, 1108 s, 1070 s, 670 (100), 438 (25). [f] Not observed.

Table 7. Selected Features (cm^{-1}) and Their Assignments in the Vibrational Spectra of Compounds **6**–**10**[a,b]

$Ph_2Te[S_2COMe]_2$ (**6**)		$Ph_2Te[S_2COEt]_2$ (**7**)		$Ph_2Te[S_2CO(i\text{-}Pr)]_2$ (**8**)		$Ph_2Te[S_2CO(n\text{-}Pr)]_2$ (**9**)		$Ph_2Te[S_2CO(n\text{-}Bu)]_2$ (**10**)		
IR[c]	Raman[d]	IR[c]	Raman[d]	IR[c]	Raman[d]	IR[c]	Raman[d]	IR[c]	Raman[d]	assgnt
1205 vs	*g*	1198 s	*g*	1208 vs	*g*	1187 m	*g*	1185 s	*g*	$\nu(S_2COC)_a$[e]
1141 s	*g*	1106 s	*g*	1084 vs	*g*	1132 m	*g*	1122 s	*g*	$\nu(S_2COC)_b$[e]
1041 vs	1038 (10)	1030 vs	1025 (25)	1020 vs	1027 (20)	1039 s	1034 (40)	1034 vs, br	1033 (40)	$\varrho(S_2COC)_c$[e]
g	998 (20)	*g*	999 (55)	*g*	997 (15)	*g*	996 (75)	*g*	997 (40)	*p*-phenyl
724 ms	*g*	724 ms	*g*	731 ms	*g*	728 ms	*g*	728 s	*g*	*f*-phenyl
678 m	*g*	678 ms	683 (5)	686 m	*g*	684 m	*g*	683 ms	683 (10)	*v*-phenyl
621 w, sh	627 (30)	*g*	671 (35)	*g*	682 (10)	650 w, sh	655 (30)	650 w, sh	654 (15)	$\nu(S_2COC)_4$[e]
450 ms, br	461 (5)	442 ms, br	460 (5)	455 ms	455 (5)	449 m	457 (15)	449 ms, br	450 (5)	*y*-phenyl[f]
g	455 (5)	*g*	439 (5)	*g*	447 (5)	433 m	430 (10)	*g*	428 (5)	δ(COC)
352 s, br	369 (100)	350 w	330 (100)	388 mw	357 (80)	357 ms	365 (100)	363 m	365 (100)	$\nu(Te-S)_{asym}$
273 mw	275 (35)	271 m	274 (30)	299 s	310 (100)	296 m	296 (20)	297 m	290 (40)	$\nu(Te-S)_{sym}$

[a] Parentheses denote relative intensities in the Raman effect. [b] s = strong, m = medium, w = weak, sh = shoulder, br = broad, and v = very. [c] Run neat between KBr plates down to 400 cm^{-1} and between polyethylene below 400 cm^{-1}. [d] Run neat in sealed capillaries. [e] In the xanthate salts, KS_2COR, these appear for R = Me at 1187 s, 1109 vs, 1049 vs, 620 (100), 476 (30); for R = Et at 1143 s, 1105 vs, 1050 s, 666 (100), 450 (55); for R = *i*-Pr at 1135 s, 1084 vs, 1056 vs, 660 (100), 462 (60); for R = *n*-Pr at 1150 s, 1117 vs, 1068 s, 659 (100), 454 (70); and for R = *n*-Bu at 1147 s, 1108 s, 1070 s, 670 (100), 438 (25). [f] X-sensitive mode. [g] Not observed.

symmetric Te–S stretching vibrations in the regions 368–393 and 279–315 cm^{-1}, respectively. The large splitting of these modes is typical of those noted for $Me_2Te[S_2POGO]_2$ compounds[38] and is consistent with an angle appreciably greater than 90°, in the case of **1** and **2** 165.90(3)[8] and 166.39(5)°, respectively. The CTeC deformation is characteristically observed in the range 199–219 cm^{-1} for all compounds in both the infrared and Raman spectra. For the diphenyl derivatives, the assignments of peaks attributable to the S_2COR groups are essentially in locations identical to those of the assignments for their dimethyl analogues, suggesting that the environments of the xanthates in the solid state are identical for the corresponding methyl and phenyl derivatives. Additional peaks in the spectra that essentially act as fingerprints for the presence of the diphenyl groups are assigned in Table 7 in accord with the Whiffen convention.[39] There are of course no isolated features attributable to Te–C modes in the diphenyl derivatives, and the Te–S stretching vibrations are only tentatively assigned because, although the ranges to which they are assigned are the same as those found for compounds **1**–**5**, the relative intensities and positions of peaks for pairs of analogous compounds are not as consistent as might be expected.

NMR Spectra. The ^1H, $^{13}C\{H\}$, and ^{125}Te NMR spectral data for compounds **1**–**10** are presented in Table 8 and 9. All of the spectra were recorded immediately after dissolution of the compounds in $CDCl_3$. The ^1H NMR spectra confirm that, for the dimethyl derivatives, $Me_2Te[S_2COR]_2$, **1**–**5**, the products are over 98% pure relative to any hydrogen-containing impurities, and all peaks have the fine structure and relative intensities expected for the presence of bis-substituted species. However, additional peaks are observed if the spectra of the same solution are re-recorded after a time delay. These peaks are readily assignable to the compounds that result from reductive elimination, namely Me_2Te (1.72 ppm) and the appropriate diligand species $ROCS_2S_2COR$ (see footnote *d* to Table 8 for data for R = Me, Et, *i*-Pr, *n*-Pr, and *n*-Bu, respectively). As the peaks assignable to Me_2Te and the diligand grow, so those assigned to $Me_2Te[S_2COR]_2$ diminish and eventually disappear after approximately 1–2 weeks. For the compounds $Ph_2Te[S_2COR]_2$, **6**–**10**, peaks of low intensity assignable to the diligands as described above and to Ph_2Te are often evident along with those assignable to compounds **6**–**10** even in spectra run as soon as the compounds are dissolved. After a matter of 2–3 days at room temperature, the peaks attributable to **6**–**10** have essentially disappeared. The difference in the rates of decomposition are illustrated by Figures 1 and 2, as discussed earlier, and the Arrhenius parameters for **4**, **5**, **7**, and **9** are given in the Experimental Section.

The chemical shifts of the methyl groups attached to tellurium are essentially identical (sharp singlet at 2.52–2.53 ppm) for all of the $Me_2Te[S_2COR]_2$ species regardless of the nature of R. The shifts are very similar (approximately 0.06 ppm downfield) to those reported for $Me_2Te[S_2CNR_2]_2$ species,[3]

(38) Drake, J. E.; Mislankar, A. G.; Ratnani, R. *Can. J. Chem.* **1994**, *72*, 1328.
(39) Whiffen, D. H. *J. Chem. Soc.* **1956**, 1350.

Table 8. ^{1}H and ^{125}Te NMR Chemical Shifts for the Dimethyl- and Diphenyltellurium Dithiocarbonates **1**−**10**[a−c]

compound	Te−CH_3/C_6H_5	O−CH_3/CH_2[d]	OC−CH_3/CH_2[d]	OCC−CH_3/CH_2[d]	^{125}Te
$Me_2Te[S_2COMe]_2$ (**1**)	2.55 (6 H, s)	4.12 (6 H, s)			482
$Me_2Te[S_2COEt]_2$ (**2**)	2.53 (6 H, s)	4.55 (4 H, q) [7.2]	1.39 (6 H, t) [7.2]		475
$Me_2Te[S_2CO(i\text{-}Pr)_2]$ (**3**)	2.52 (6 H, s)	5.64 (2 H, sept) [6.0]	4.03 (12 H, d) [6.0]		475
$Me_2Te[S_2CO(n\text{-}Pr)]_2$ (**4**)	2.53 (6 H, s)	4.45 (4 H, t) [6.9]	1.78 (4 H, m) [6.9], [6.9]	0.97 (6 H, d) [6.9]	477
$Me_2Te[S_2CO(n\text{-}Bu)]_2$ (**5**)[e]	2.53 (6 H, s)	4.51 (4 H, t) [6.6]	1.76 (4 H, m) [6.6], [7.3]	1.42 (4 H, m) [7.3], [7.2]	478
$Ph_2Te[S_2COMe]_2$ (**6**)[f]	7.93−7.90, 7.50−7.40 (10, H)	4.02 (6 H, s)			758
$Ph_2Te[S_2COEt]_2$ (**7**)[f]	7.91−7.88, 7.50−7.39 (10, H)	4.46 (4 H, q) [7.2]	1.37 (6 H, t) [7.2]		758
$Ph_2Te[S_2CO(i\text{-}Pr)]_2$ (**8**)[f]	7.92−7.89, 7.49−7.38 (10, H)	5.56 (2 H, sept) [6.3]	1.34 (12 H, d) [6.3]		756
$Ph_2Te[S_2CO(n\text{-}Pr)]_2$ (**9**)[f]	7.95−7.92, 7.48−7.42 (10, H)	4.40 (4 H, t) [6.6]	1.79 (4 H, m) [6.6], [7.2]	0.99 (6 H, t) [7.2]	759
$Ph_2Te[S_2CO(n\text{-}Bu)]_2$ (**10**)[e,f]	7.93−7.89, 7.48−7.37 (10, H)	4.42 (4 H, t) [6.6]	1.73 (4 H, m) [6.6], [7.3]	1.40 (4 H, m) [7.3], [7.2]	759

[a] The spectra were recorded in $CDCl_3$ and reported in ppm from Me_4Si for ^{1}H and in ppm from Me_2Te for ^{125}Te. [b] Number of protons and multiplicities are in parentheses (s = singlet; t = triplet; d = doublet; q = quartet; sept = septet; m = multiplets). [c] Coupling constants in Hz shown in square brackets. [d] Peaks attributable to the diligands are seen for $[MeOCS_2]_2$ at 4.21 (6 H, s); for $[EtOCS_2]_2$ at 4.66 (4 H, q), 1.45 (6 H, t); for $[(i\text{-}Pr)OCS_2]_2$ at 5.65 (2 H, sept), 1.41 (12 H, d); for $[(n\text{-}Pr)OCS_2]_2$ at 4.55 (4 H, t), 1.85 (4 H, m), 1.04 (6 H, t); and for $[(n\text{-}Bu)OCS_2]_2$ at 4.58 (4 H, t), 1.79 (4 H, m), 1.45 (4 H, m), 1.01 (6 H, t). [e] Peaks corresponding to OCCC−CH_3 for **5** are seen centered at 0.93 (6 H, t) [7.2] and for **10** at 0.95 (6 H, t) [7.2]. [f] Peaks corresponding to the presence of Ph_2Te are also seen at approximately 7.65−7.62, 7.28−7.15 in the ^{1}H NMR spectra of **6**−**10** and at 692.0 in their ^{125}Te NMR spectra.

Table 9. ^{13}C NMR Chemical Shifts of the Dimethyl- and Diphenyltellurium Dithiocarbonates **1**−**10**[a]

		$(C_6H_5)_2Te$[b]				[S_2COR][c]				
compound	$(CH_3)_2Te$	C_1	$C_{2,6}$	C_4	$C_{3,5}$	S_2CO	S_2COC	S_2COCC	S_2COC_2C	S_2COC_3C
$Me_2Te[S_2COMe]_2$ (**1**)	15.57					220.98	60.97			
$Me_2Te[S_2COEt]_2$ (**2**)	15.54					220.13	70.83	14.11		
$Me_2Te[S_2CO(i\text{-}Pr)]_2$ (**3**)	15.51					219.37	78.70	21.53		
$Me_2Te[S_2CO(n\text{-}Pr)]_2$ (**4**)	15.57					220.31	76.47	21.95	10.60	
$Me_2Te[S_2CO(n\text{-}Bu)]_2$ (**5**)	15.55					220.32	74.88	30.52	19.30	13.83
$Ph_2Te[S_2COMe]_2$ (**6**)		135.08	132.33	130.91	129.71	220.07	60.26			
$Ph_2Te[S_2COEt]_2$ (**7**)		135.01	132.07	130.87	130.13	219.29	70.35	14.24		
$Ph_2Te[S_2CO(i\text{-}Pr)]_2$ (**8**)		134.87	131.82	130.95	130.14	218.94	78.41	21.54		
$Ph_2Te[S_2CO(n\text{-}Pr)]_2$ (**9**)		135.09	132.36	130.85	130.14	219.52	75.95	22.45	10.96	
$Ph_2Te[S_2CO(n\text{-}Bu)]_2$ (**10**)		135.05	132.33	130.79	130.12	219.48	74.29	30.92	19.72	14.36

[a] The spectra were recorded in $CDCl_3$ and reported in ppm from Me_4Si. [b] Peaks arising from Ph_2Te are seen in the spectra of **6**−**10** at approximately 138.1, 129.7, 128.0, and 115.0 [c] Peaks attributable to the diligands are seen for $[MeOCS_2]_2$ at 208.26, 61.81; for $[EtOCS_2]_2$ at 207.42, 71.71, 13.90; for $[(i\text{-}Pr)OCS_2]_2$ at 206.93, 80.38, 21.26; for $[(n\text{-}Pr)OCS_2]_2$ at 206.78, 76.88, 22.28, 10.85; and for $[(n\text{-}Bu)OCS_2]_2$ at 206.73, 75.29, 30.60, 19.72, 13.83.

which is consistent with the presence of ligands of similar anisodenticity. The xanthate ligands give the expected first-order spectra, except of course for the central CH_2 groups in the *n*-propyl and *n*-butyl groups. In general, the chemical shifts are similar regardless of whether the xanthate is attached to the Me_2Te or the Ph_2Te moiety, consistent with the xanthates having similar anisobidentate linkages in all 10 derivatives.

In the ^{13}C NMR spectra, the chemical shifts of the ligand methyl, ethyl, isopropyl, *n*-propyl, and *n*-butyl derivatives are relatively the same regardless of whether methyl or phenyl groups are attached to tellurium or the number of such groups (Table 9). Also, comparison with the diligand spectra, resulting from the reductive elimination, indicates similar values for the chemical shifts of all the alkyl carbon atoms, which in turn are close to the values of the starting salts. The peak that is shifted distinctly is that associated with the thio-carbon atom. The S_2CO peak is seen at approximately 233 ppm for the potassium salts, 207 ppm for the diligands, and in the range 218.94−220.98 ppm for compounds **1**−**10**. It seems reasonable to assume that the salt represents values to be expected for a bidentate ligand and the diligand values expected for a monodentate lignad so that those for **1**−**10** are consistent with all of these compounds containing anisobidentate ligands as found in the structures of **1** and **2**. The consistent nature of the bonding, regardless of the organoxanthate group, is also indicated by the essentially constant value for the chemical shifts of the H_3C−Te carbon atoms which cover the range 15.51−15.57 ppm for all five dimethyl derivatives. These values can be compared to those for $Me_2Te[S_2CNMe_2]_2$ (16.6 ppm), which presumably reflects similar values of effective electronegativity for xanthates and dithiocarbamates, as well as similar orientations toward tellurium and hence similar xanthate environments in **1**−**10** regardless of the nature of the organic group in the xanthate or attached to tellurium.

The ^{125}Te NMR chemical shifts, which are presented in Table 8, fall in the range 475−482 ppm for Me_2Te in the $Me_2Te[S_2COR]_2$ species **1**−**5**. These shifts are similar to those of 463 and 475 ppm reported for $Me_2Te[S_2CNMe_2]_2$ and $Me_2Te[S_2CNEt_2]_2$, respectively. The dithio-ligand species, Me_2TeL_2, form the beginning of a series with the halides Me_2TeI_2, 520, Me_2TeBr_2, 649, and Me_2TeCl_2, 734 ppm. The chemical shifts for the $Ph_2Te[S_2COR]_2$ species **6**−**10** also fall over a narrow range (756−759 ppm). These values are again slightly larger than those of the dithiocarbamate analogues and approximately 250 ppm less than the chemical shift of the dichloride, Ph_2TeCl_2 (917 ppm). However the similarities in the ^{125}Te chemical shifts in the Me_2TeL_2 and Ph_2TeL_2 series do not extend to the reductive-elimination products Me_2Te and Ph_2Te. The chemical shifts for $Ph_2Te[S_2COR]_2$ species are less than 70 ppm from Ph_2Te (690 ppm), which is nearly an order of magnitude less than the difference between the chemical shifts of the more stable dimethyl derivatives and Me_2Te (0 ppm). This could indicate that in solution the Ph_2TeL_2 species undergo rapid exchange, resulting in an equilibrium position whose magnetic environment is closer to that of Ph_2Te, possibly by alternating bonded and anisobonded S atoms. This would be consistent with the slight differences in the orientation of the dithiocarbonate groups in **2** and **7** and the indication that the lone pair might be stereochemically inactive in the case of **7**. Such an environment would differ from one in which the equilibrium was closer to that of the solid state structure of **2**, which appears to involve a stereochemically active lone pair whether the

intramolecular Te--S links are included in the coordination sphere or not. This could account for the difference in activation energies between $Me_2Te[S_2COR]_2$ and $Ph_2Te[S_2COR]_2$ of 10−15 kJ mol^{-1}. For **6**−**10**, the peak attributable to Ph_2Te is evident in the initial ^{125}Te NMR spectra because the normal collection time of up to 60 min per spectrum is sufficiently long to ensure reductive elimination is underway. The sensitivity is such that normally after 1 day the peaks attributable to the $Ph_2Te[S_2COR]_2$ species have disappeared and only that attributable to Ph_2Te remains. By contrast, for compounds **1**−**5**, the initial ^{125}Te NMR spectra do not show a peak attributable to Me_2Te and the peaks attributable to the $Me_2Te[S_2COR]_2$ species are not totally lost for at least 1−2 weeks.

Acknowledgment. We wish to thank the Natural Sciences and Engineering Research Council of Canada for financial support. L.N.K. expresses thanks for an NSERC Research Reorientation Associateship.

Supplementary Material Available: Tables SI−SV listing experimental details, anisotropic thermal parameters of non-hydrogen atoms, and final fractional coordinates and thermal parameters for hydrogen atoms (5 pages). Ordering information is given on any current masthead page. Structure factor tables may be obtained directly from the authors.

IC940797T